SCATTER IN THE CLEAVAGE FRACTURE TOUGHNESS OF A533B PLATE

D.A. Curry, I. Milne and K.N. Akhurst*

The fracture toughness of A533B pressure vessel steel plate has been measured over the temperature range -100°C to +20°C. The final failure mode was cleavage in all cases, but in some specimens ductile crack growth preceded fracture. A very large scatter in toughness was observed. Microstructural examination revealed bands with much finer prior austenite grain sizes and carbide dispersions than the matrix. These bands had higher hardness and substantially higher carbon and molybdenum concentrations than the matrix. Uncertainties about three dimensional aspects of the cleavage fracture process prevent any quantitative assessment of the influence of the segregated bands on the observed scatter in toughness.

INTRODUCTION

Fracture toughness tests performed on one material under nominally identical conditions invariably give a range of results which is greater than that associated with inaccuracies in the test technique. This scatter in toughness can be particularly pronounced in the case of heavy section structural steels. It gives rise to considerable uncertainty in any structural defect tolerance calculations, for which it is generally necessary to adopt a lower bound toughness value. An understanding of the microstructural sources of the scatter will aid the definition of a lower bound to toughness data as well as being of obvious benefit in any attempt to reduce the scatter in toughness.

This paper presents the results of toughness tests performed on one plate of A533B pressure vessel steel. The scatter in the cleavage fracture toughness is large. Microstructural examination of the plate revealed substantial fine scale banding. The significance of these bands as possible sources of scatter in cleavage toughness is discussed.

FRACTURE TOUGHNESS

This study concerned a 130 mm thick plate of A533B Class 1 pressure vessel steel. It had been cross rolled to its final thickness, prior to its quenching and tempering heat treatment. The plate was subjected to a further heat treatment of 3 hrs at 600°C to simulate the effects of post weld stress relief.

Test Details

Fracture toughness tests were performed on 25 mm and 50 mm compact tension (CT) specimens and 125 mm square single edge notched bend (SENB) specimens. They were aligned (L/ST) so that the crack propagated through the plate

*Central Electricity Research Laboratories, Kelvin Avenue, Leatherhead, Surrey

thickness. They were fatigue pre-cracked at room temperature with a maximum stress intensity factor of 20 $MPam^{\frac{1}{2}}$ to an initial crack length to specimen width ratio of $\sim$0.5. The specimens were tested at a displacement rate of 0.01 mm sec^{-1} in the temperature range $-100^{o}C$ to $+ 15^{o}C$. The initial crack length and the extent of any ductile crack growth were measured for each specimen after testing by weighing the appropriate portion of a fractograph. Thus the crack lengths and crack growth increments quoted are area based averages rather than the averages of a number of spot measurements.

The value of the J contour integral at fracture was estimated using the expression:

$$J_o = \frac{U}{B(W - a)} f(\frac{a}{w}) \qquad (1)$$

For those specimens which displayed ductile crack growth prior to cleavage instability, the J_o values were corrected to allow for crack growth as:

$$J_R = J_o \left\{ 1 - \Delta a \frac{(0.75 f(\frac{a}{w}) - 1)}{W - a} \right\} \qquad (2)$$

Finally a critical stress intensity factor, K_{JC}, was calculated in the conventional manner from J_o or J_R as appropriate:

$$K_{JC} = \left\{ \frac{J E}{1 - \nu^2} \right\}^{\frac{1}{2}} \qquad (3)$$

Toughness Results

K_{JC} values are shown as a function of temperature in Figure 1. In some specimens ductile crack growth preceded final cleavage fracture - the results for these specimens are indicated by open symbols, whereas filled symbols are used for specimens in which fracture was exclusively by cleavage. Tensile properties for this plate have been reported elsewhere (1). These have been used to assess the validity of the toughness tests. All specimens were too small to satisfy the British Standard size requirements for plane strain fracture toughness K_{IC} tests (2). Most of the specimens did, however, meet the size requirements for J_{IC} testing (3):

$$a, B, (W - a) > 25 J_{o,R}/\sigma_{flow} \qquad (4)$$

On Figure 1, bracketted points indicate specimens which did not satisfy equation (4).

The occurrence of ductile tearing in some specimens prior to the cleavage instability should not be thought of as invalidating the K_{JC} result. It merely reflects the high resistance to cleavage fracture of the specimens in question. The increase in toughness associated with ductile crack growth allows the applied J to increase up to the critical value for cleavage, (4).

The scatter in toughness, K_{JC}, at any one temperature is considerable and becomes more pronounced towards the upper end of the range of test temperatures. For example, at $0^{o}C$ one 50 mm CT specimen failed without any measurable plastic displacement at a K_{JC} of 137 $MPam^{\frac{1}{2}}$ whilst another notionally identical specimen failed after gross yielding and 2.87 mm ductile-crack growth at a K_{JC} well in excess of 500 $MPam^{\frac{1}{2}}$. Within the scatter there is a clear trend to increasing K_{JC} with increasing test temperature. The results for the 25 mm CT specimens tend to lie in the upper half of the scatter band whilst the mean K_{JC} for the 50 mm CT specimens seems to be in the lower half. All test results for 125 mm square bend specimens fall towards the lower end of the scatter band. Thus, despite the considerable scatter, there is limited evidence of an increase in K_{JC} with decreasing specimen size.

Together with the toughness data, the ASME reference curve for K_{IC} (5) is shown in Figure 1:

$$K_{IC}(T) = 1.1 \{33.2 + 2.81 \exp 0.036(T - RT_{NDT} + 56)\} \tag{5}$$

$$RT_{NDT} = T_{68} - 33$$

where T_{68} is the temperature of the 68 Joule Charpy energy level. This has been reported elsewhere as -6°C for this plate (6). Note that in Figure 1 the ASME K_{IC} reference curve has been extended to much higher levels of toughness than the 200 $MPam^{\frac{1}{2}}$ ductile cut off defined by ASME, and that none of the toughness tests met the K_{IC} size requirements. Nevertheless, all the tests results lie above the K_{IC} reference curve, regardless of the incidence of ductile crack growth prior to cleavage fracture.

MICROSTRUCTURE

The plate had been subjected to a stress relieving heat treatment of 3 hours at 600°C in addition to its initial quenching and tempering heat treatment. The resulting tempered granular bainitic microstructure is shown in Figure 2 (2% nital etch). The prior austenite grain boundaries were somewhat irregular and there were large local variations in the prior austenite grain size (ASTM 3-10). Etching in saturated aqueous picric acid/teepol revealed that the fine grained regions, which lay in narrow bands aligned in the principal rolling direction, contained a much finer carbide particle dispersion than the bulk of the plate (Figures 3 and 4). These bands were typically 50-100 μm wide and 1 mm long when viewed in the long transverse direction. They were less well defined on the plane perpendicular to the principal rolling direction, indicating that the cross rolling of the plate had not been fully effective.

A microhardness survey was conducted across one of the bands (Figure 4). Vickers hardness values are marked on each indent. These show, as expected, that the finer microstructure of the band produced a higher hardness than that of the matrix - a peak H_v of 274 as opposed to the matrix range of 210-220.

The chemical composition of this band was investigated along the line of the microhardness traverse by X-ray spectrometry. The peak concentration across the band is given in Table 1 for the major alloying elements, together with the bulk composition. It is clear that both carbon and molybdenum were strongly segregated into the band and that the band was enriched, to a lesser degree, in manganese and silicon. There was little obvious segregation of nickel or chromium.

TABLE 1 - Concentrations of Major Alloying Elements in A533B Plate under Study

Element	C	Mn	Ni	Mo	Si	Cr
Bulk Concentration wt.%	0.16	1.39	0.63	0.51	0.22	0.10
Peak Concentration in Segregated Band wt.%	0.35	1.74	0.69	0.82	0.31	0.125

DISCUSSION

The A533B plate studied displayed substantial scatter in cleavage fracture toughness and there were pronounced local inhomogeneities in the chemical composition and microstructure. It seems highly probable that the presence of the segregate bands was responsible, at least in part, for the scatter in toughness. However, the comparatively small size of the bands made it impossible to associate any particular toughness level with their presence at the crack tip.

It is possible (7) to relate the fracture toughness of a ferritic steel to microstructurally determined parameters by the application of the Ritchie, Knott and Rice (8) cleavage fracture criterion:

$$K_{IC} = \beta^{\left(\frac{N+1}{2}\right)} X_o^{\frac{1}{2}} \frac{\sigma_f^{\left(\frac{N+1}{2}\right)}}{\sigma_y^{\left(\frac{N-1}{2}\right)}} \qquad (6)$$

For A533B, N is typically ~ 8 (9). Thus, if the local yield stress is taken as being proportional to the hardness, the hardness difference between the matrix and the bands is of itself sufficient to explain most of the spread in toughness values observed at any one temperature. There will also be fluctuations in both the characteristic distance and the cleavage fracture stress associated with the microstructural inhomogeneities which could tend to increase further the scatter in the local values of fracture toughness. It is of interest that the sensitivity of the fracture toughness to local fluctuations in yield stress, fracture stress and characteristic distance is predicted by equation 6 to increase with decreasing work hardening rate (increasing N). Such an analysis, of course, neglects the influence of local hardness changes on the form of the crack tip stress distribution.

The characteristic distance, which may be thought of as describing the minimum volume of material in which the cleavage fracture process can operate, is usually of the order of a few grain diameters. Parks (10) found the characteristic distance in an A533B plate to be about 75 μm, whereas Green (11) determined a lower value, 32 μm, for an essentially similar bainitic steel. The segregated bands observed in the current study have dimensions which in all directions are at least comparable with the characteristic distance. They are, therefore, sufficiently wide to contribute in a significant manner to the fracture process.

It is tempting to speculate on the effect of reducing the width of the bands, perhaps by further hot rolling, on the fracture properties of the plate. By making the bands much smaller in one direction than the characteristic distance, would they be precluded from causing cleavage fracture so that the scatter in fracture toughness would be reduced for that crack propagation direction? The outcome would seem to depend upon the physical significance of the characteristic distance. If it does indeed define the minimum volume of material in which the fracture process can operate, then the effect described above would be observed. An alternative interpretation of the characteristic distance is that it represents the statistical competition between different sized crack nuclei ahead of the main crack tip (12). In this case reducing the band width to less than the characteristic distance would reduce the maximum possible contribution to the failure probability from the segregated material. That is to say the maximum divergence from the matrix toughness would decrease, but the bands would still be capable of influencing the fracture toughness displayed by the plate. Thus it can be deduced that a reduction in the width of the segregated bands to below the characteristic distance should at least reduce the scatter in cleavage toughness for cracks propagating perpendicular to the plate rolling plane.

The preceding discussion ignores the three dimensional nature of the fracture process. Does cleavage fracture occur when the applied stress intensity factor first exceeds the lowest local toughness value, determined by the micromechanism outlined above? i.e. is the 'weakest-link' hypothesis (13) applicable? Alternatively, does the material as a whole display a toughness equal to the mean of all toughness values along the crack front? Hagiwara and Knott (14) have proposed a model for the cleavage fracture of mixed microstructure materials based on the latter fracture criterion. This predicts the probability of a given fracture toughness from the distribution of fracture toughness for each component and the volume fractions of the component microstructures. Unfortunately the information necessary to apply this model to the current results is not available.

Another three dimensional aspect of the cleavage fracture micromechanism that merits attention is the possible occurrence of isolated cleavage microcracks at different points along the crack front before final fracture. When the local microstructure allows the formation of a cleavage crack at an applied stress intensity factor well below the mean fracture toughness, that crack may only propagate across one or two grains before arresting at a crystallographic discontinuity such as a grain boundary. Further crack extension then requires the nucleation of fresh cracks in the adjacent grains. Such isolated cleavage microcracks have been observed by Khan, Shoji and Takahashi (15) to precede final cleavage fracture in several low alloy ferritic steels. Plainly the occurrence of these microcracks indicates that the "weakest link" hypothesis is inappropriate, at least on a microscopic scale. Furthermore, it will mean that the macroscopic fracture criterion is no longer the attainment of the mean toughness along the crack front. Instead local 'load-shedding' will occur and the situation becomes analogous to the fracture of a bundle of fibres, as described by McCartney (16). In this case, however, the bundle of fibres (the array of grains ahead of the crack tip) is subjected to a severe stress gradient in the direction of crack propagation.

CONCLUSIONS

1. The cleavage fracture toughness of a plate of A533B pressure vessel steel displayed substantial scatter.

2. There are fine bands of segregated material aligned parallel to the rolling direction. These have higher molybdenum and carbon contents than the matrix, smaller prior austenite grain sizes and higher microhardness levels.

3. These segregate bands probably contribute to the scatter observed in fracture toughness. However, uncertainty about three dimensional aspects of the cleavage fracture micromechanism precludes any quantification of their influence on the scatter.

4. The scatter in toughness should be reduced for cracks propagating through the plate thickness if the width of the segregated bands can be reduced to less than the characteristic distance for cleavage fracture.

ACKNOWLEDGEMENT

Thanks are due to Mr A. Gofton of Midlands Region SSD for performing the bulk chemical analysis of the plate here studied. This work was performed at the Central Electricity Research Laboratories and is published by permission of the Central Electricity Generating Board.

SYMBOLS USED

a = initial crack length

B = specimen thickness

β = stress singularity amplitude

Δa = ductile crack growth

E = Young's modulus

$f(\frac{a}{w})$ = calibration function tabulated in ASTM E813

J_o = critical J value if no ductile crack growth

J_R = critical J value corrected for ductile crack growth

K_{IC} = plane strain fracture toughness

K_{JC} = critical stress intensity factor calculated from J_o or J_R

N = Ramberg-Osgood strain hardening coefficient

ν = Poisson's ratio

σ_f = cleavage fracture stress

σ_{flow} = flow stress

σ_y = yield stress

U = total energy input to toughness specimen

W = specimen width

X_o = characteristic distance

REFERENCES

1. Milne, I. and Curry, D.A., 1980, "Fracture toughness and crack growth resistance of submerged arc and manual metal arc weldments in A533B plate", Proc. 4th In. Conf. on Pressure Vessel Technology, London, Inst. Mech. Eng.

2. British Standards Institution, BS5447 - 1977, "Methods of plane strain fracture toughness (K_{IC}) testing".

3. ASTM, E813 -81, "The determination of J_{IC}, a measure of fracture toughness"

4. Milne, I. and Curry, D.A., 1981, "Ductile crack growth analysis within the ductile-brittle transition regime: predicting the permissible extent of ductile crack growth", CEGB Report No. RD/L/2209N81

5. ASME, 1977, Boiler and pressure vessel codes, Section III Article NB2331 and Section XI Appendix A, Article A4000

6. Milne, I. and Curry, D.A., 1979, "Charpy energy transitions for weld metal and heat affected zones in SA533B Class 1 plate", in "Mechanical Behaviour of Materials", eds. K.J. Miller and R.F. Smith, 3 p415, Pergamon Press, Oxford

7. Curry, D.A., 1978, Nature, 276, 50

8. Ritchie, R.O., Knott, J.F. and Rice, J.R., 1973, J. Mech. Phys. Sol., 21, 395

9. Milne, I., 1981, "Failure assessment diagram and J estimates - a comparison for ferritic and austenitic steels", CEGB Report No. RD/L/2208N81

10. Parks, D.M., 1976, J. Eng. Mater. Technol., 98, 30

11. Green, G., 1975, Ph.D Thesis, Univ. of Cambridge

12. Curry, D.A. and Knott, J.F., 1979, Met. Sci., 13, 341

13. Wiebull, W., 1939, Proc. Ing. Veteenskapsakad, No. 151

14. Hagiwara, Y. and Knott, J.F., 1981, "Cleavage fracture in mixed microstructures" in "Advances in Fracture Research", ed. D. Francois, Vol. II p. 707, Pergamon Press, Oxford

15. Khan, M.A., Shoji, T. and Takahashi, M., 1982, Met. Sci., 16, 118

16. McCartney, L.N., 1980, "Statistics for the static strength of fibre bundles", in Proc. Conf. "Micromechanisms of Crack Extension (Mechanics and Physics of Fracture II)", Cambridge, Metals Soc. and Inst. Physics.

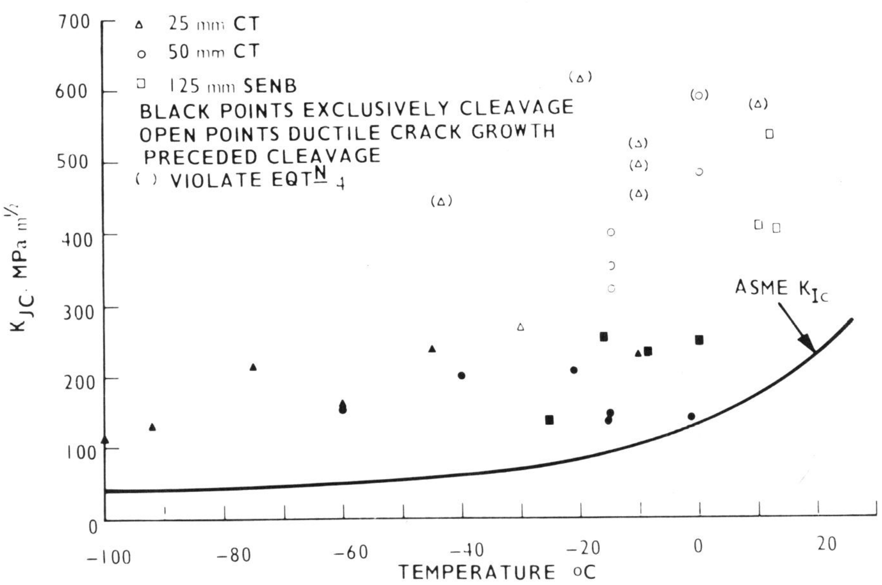

Figure 1 Temperature dependence of cleavage toughness K_{JC}

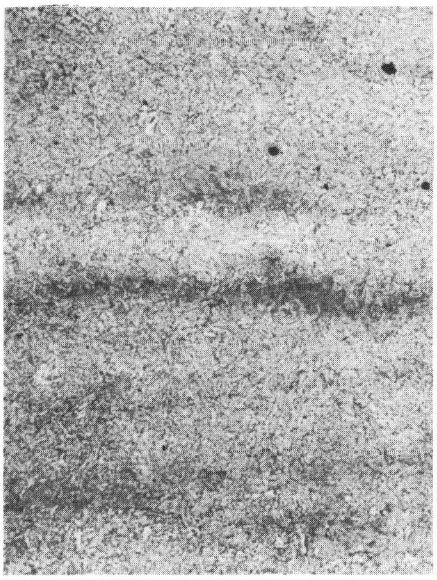

Plate Microstructure

Figure 2 Nital etch ×250

Figure 3 Picric acid/teepol etch ×100

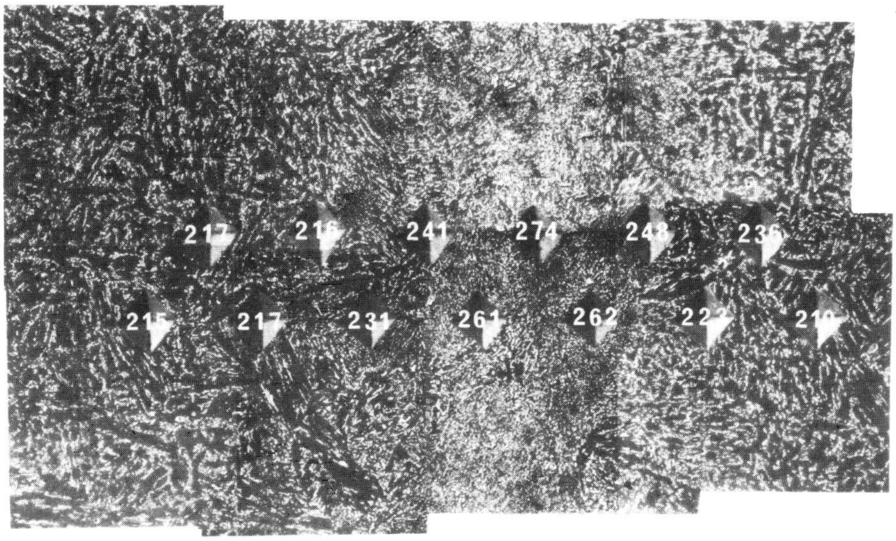

Figure 4 Microhardness traverse, picric acid/teepol etch ×500